

## Relativistic self-focusing and channel formation in laser-plasma interactions

Burke Ritchie

University of California, Lawrence Livermore National Laboratory, Livermore, California 94550

(Received 28 March 1994)

Nonparaxial wave propagation theory is used to study relativistic self-focusing and channel formation in the propagation of an intense, short-pulse laser through an underdense plasma. The stable on-axis channel predicted by paraxial theory is found to break up into on-axis channel remnants and off-axis rings.

PACS number(s): 52.40.Nk

Currently there is much interest in the propagation of an intense laser pulse through a plasma. The interaction accelerates the electrons to relativistic energies. The behavior of a single electron in the presence of a laser field has long been studied both in quantum [1] and classical dynamics [2]. More recently, from the point of view of the design of a practical device such as a wake-field particle accelerator, theorists [3] have studied laser interaction with an underdense plasma, in which the electrons collectively respond as a fluid. Other theorists [4], concerned with nuclear fusion, have studied laser interaction with an overdense plasma, in which the electron response is modeled by particle-in-cell theory.

Sun *et al.* [5] used a relativistic Maxwell-fluid model to predict relativistic self-focusing and channel formation in the passage of an intense laser pulse through a preformed plasma. The result is based on the dynamical behavior of the fluid on average over one optical cycle, whereupon ponderomotive exclusion and electrostatic restoring forces are predicted to be in equilibrium. More recently Borisov *et al.* [6] have performed extensive modeling calculations based on this theory [5], and an experiment [7] on the observation of self-channeling has been reported.

In addition to the cycle-average approximation to the fluid dynamics the theoretical result depends on the paraxial-wave approximation to Maxwell's equation. However, quite generally Feit and Fleck [8] have shown that the paraxial approximation breaks down in a region of strong self-focusing because the beam undergoes wide-angle scattering, as required by the wave uncertainty principle when the beam diameter becomes small, i.e., of the order of the optical wavelength. Retention of the full rather than the transverse Laplacian in the scalar wave equation makes scattering through the entire  $\pi$  rad possible. In their model [8] approximations are made such that the maximum scattering angle is  $\pi/2$  rad, whereupon the nearly collapsed components of the beam attenuate exponentially, i.e., these components can no longer propagate in the forward direction. This results in an abrupt on-axis power loss in the region of self-focus, bringing into question the achievement of the critical power [5,6] needed to form a stable on-axis channel. In this paper I study channel formation and beam stability using a nonparaxial theory. The method of solution is general enough so that scattering through the entire  $\pi$  rad is described. I find that nonparaxiality has a profound effect on beam shape and stability, leading eventually to beam breakup and filament formation.

The model [5,6] suitably generalized to include nonparaxiality, is described by the equations

$$\left(2i\frac{k}{c}\frac{\partial}{\partial t} + \nabla^2 + k^2 n^2\right)\mathcal{A} = 0, \quad (1a)$$

$$n^2 = 1 - \left(\frac{\omega_p}{\omega}\right)^2 \gamma^{-1} (1 + k_p^{-2} \nabla^2 \gamma), \quad (1b)$$

$$\gamma = \left(1 + \frac{1}{2} \frac{|e \cdot \mathcal{A}|^2}{m^2 c^4}\right)^{1/2}, \quad (1c)$$

where the square of the plasma frequency is defined as

$$\omega_p^2 = \frac{4\pi e^2 n_e}{m}, \quad (2)$$

where  $n_e$  is the electron density and  $k_p = \omega_p/c$ ,  $k = \omega/c$ , where  $\omega$  is the optical frequency. In Eqs. (1)  $\gamma$  is the temporally slowly varying part of the Lorentz factor consistent with the definition of the Maxwell field,

$$A = \frac{1}{2}(\mathcal{A}e^{-i\omega t} + \mathcal{A}^* e^{i\omega t}), \quad (3)$$

where we have ignored the second-order time derivative on the slowly varying envelope,  $\mathcal{A}$ . In the nonrelativistic limit, when  $\gamma = 1$ , Eq. (1b) reduces to the familiar result for the square of the refractive index from the Drude model. In Eq. (1a) the Laplacian is written in cylindrical coordinates where, for an assumed azimuthally symmetric problem, the envelope depends only on the longitudinal coordinate  $z$  and the radial coordinate  $\rho$ . The paraxial problem is recovered by rewriting Eq. (3)

$$A = \frac{1}{2}(ae^{-i\omega t + ikz} + a^* e^{i\omega t - ikz}) \quad (4)$$

and deriving the equation for the envelope  $a$  neglecting second-order  $t$  and  $z$  derivatives. In steady state, where the time derivative is zero, Eq. (1a) reduces to the Helmholtz equation studied by Feit and Fleck [8]. Rigorous treatment of the physics demands that the vector set of Maxwell equations be solved; however, as pointed out in [8] the scalar Maxwell equation describes the diffractive loss of on-axis power without explicitly accounting for where it goes.

Equations (1) are scaled to the variables  $t_s = \omega_p t$ ,  $z_s = k_p z$ , and  $\rho_s = k_p \rho$ , where the subscripts are hereafter omitted. The plasma density is  $n_e = 7.5 \times 10^{21} \text{ cm}^{-3}$  and the optical frequency is the same as that in [6], namely  $7.44 \times 10^{15} \text{ s}^{-1}$ . This corresponds to a plasma which is  $(\omega/\omega_p)^2 \sim 2.4$  times underdense, in contrast to the plasma of [6], which is about 24 times underdense. It is not feasible to

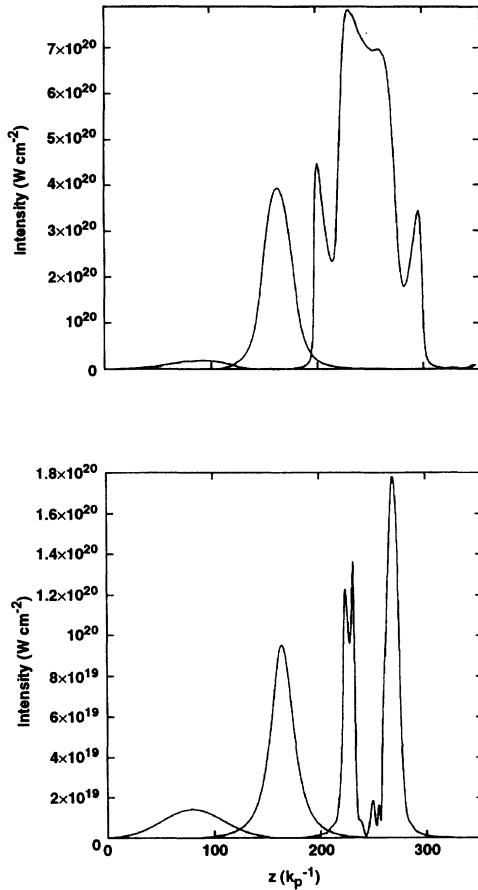


FIG. 1. Three snapshots of the on-axis intensity. Top: paraxial. Bottom: nonparaxial.

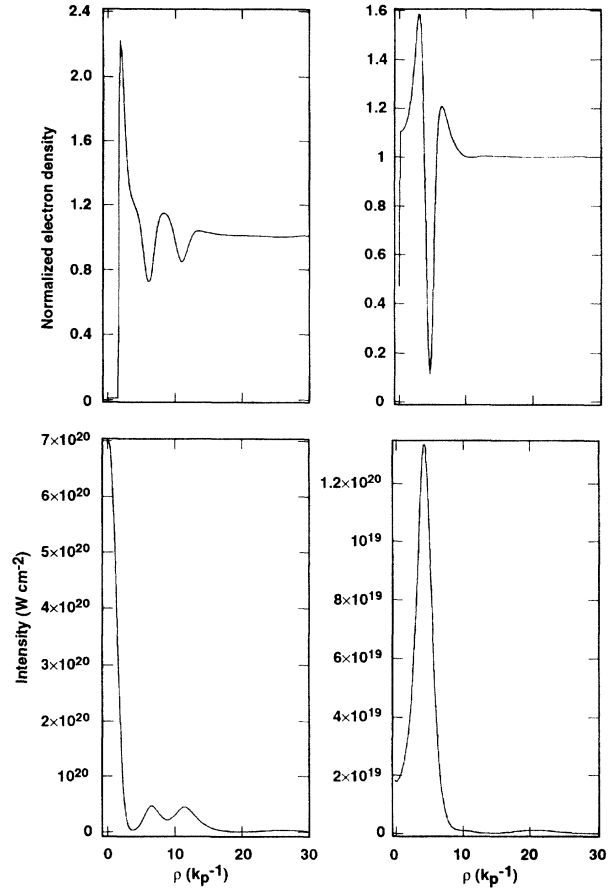


FIG. 2. Radial profiles at maximum time, i.e.,  $z = 250k_p^{-1}$  in Fig. 1. Left hand: paraxial. Right hand: nonparaxial.

solve Eq. (1a) for the latter case because of the rapid variation of the envelope  $\mathcal{A}$  along  $z$ . However, it is clear from the scaled form of Eq. (1a) that both the diffraction term and the nonlinear term of the index scale as  $\omega_p/\omega$ , so that my conclusions about the nonparaxiality of the propagation are also applicable to the more underdense case [6]. In other words, the more underdense case requires a longer propagation length before the onset of self-focusing; nevertheless the eventual reduction of the radius of the beam to the order of an optical wavelength will result in the breakdown of paraxial theory.

In paraxial theory, closeness to critical density, i.e.,  $\omega_p/\omega = 1$ , requires a lower critical power [6], i.e., the power at which self-focusing through the nonlinear index overcomes diffraction, according to the scale  $(\omega/\omega_p)^2$ . In nonparaxial theory, where the input envelope is assumed to be Gaussian in  $z$  as well as in  $\rho$  (Fig. 1), the on-axis average power is here defined as  $2\pi\rho c|\omega\mathcal{A}/c|^2/8\pi$  integrated over  $\rho$  and averaged over  $z$ . Empirically I have found this nonparaxial critical power to be about  $1.0 \times 10^{11}$  W, which, for the input pulse, is the same as the peak power at the input  $z$  point defined in the usual way (i.e., the above expression integrated over  $\rho$ ). This turns out to be more than two and one-half times the paraxial critical power given in [6]. This is reasonable because there is greater diffraction in the nonparaxial theory.

The numerical algorithm used to solve Eq. (1a) is the same as that described elsewhere [9]. The difference here is that the nonlinear index must be treated explicitly. Nevertheless the results are numerically stable. The problem is resolved by using 2001 temporal, 2001 longitudinal spatial, and 301 radial spatial grid points, respectively, for a maximum time of  $170\omega_p^{-1}$ , maximum longitudinal distance of  $350k_p^{-1}$ , and a maximum radial distance of  $60k_p^{-1}$  (Figs. 1–3). A damping term is added to the equation on the boundary edges to eliminate spurious reflection from the boundaries. The widths of the input Gaussian pulses are  $40k_p^{-1}$  in  $z$  and  $20k_p^{-1}$  in  $\rho$ . On the plasma wavelength scale the  $z$  width corresponds to a pulse length of almost 10 fs, which is in the short-end range of current short-pulse laser experiments. These widths can be increased, requiring greater machine storage, as needed to simulate the results of actual experiments.

Figures 1–3 show paraxial vs nonparaxial results. Figure 1 shows a series of snapshots beginning with the input Gaussian pulse and ending at the maximum time ( $170\omega_p^{-1}$ ). The input pulse is centered on the  $z$  scale at  $80k_p^{-1}$  and is assumed to be surrounded by a preformed plasma. The experimental conditions for producing the plasma by ionization of neutral atoms [10] or for propagating through a vacuum-plasma interface in the case of a preformed plasma will not be treated here. Figure 2 shows the radial profile of the nor-

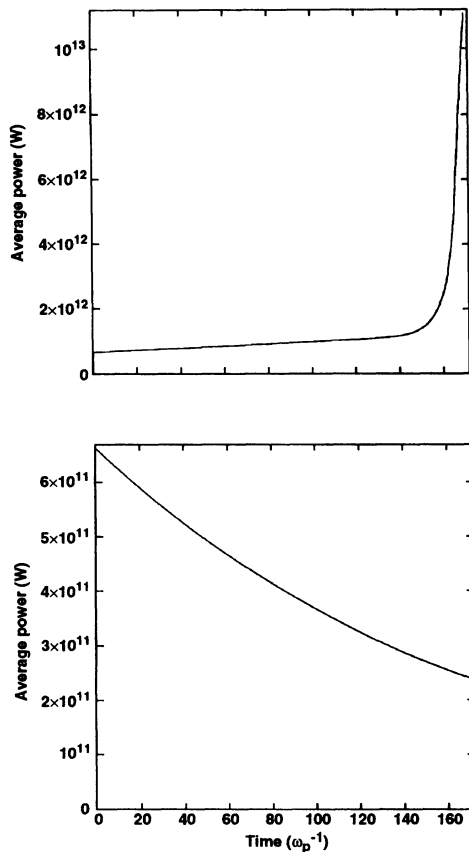


FIG. 3. Average on-axis power. Top: paraxial. Bottom: nonparaxial.

malized electron density and pulse at maximum time or at  $(80+170)k_p^{-1}$  on the  $z$  scale.

In paraxial theory the pulse widens in  $z$  (Fig. 1) as it collapses in  $\rho$  (Fig. 2). This unphysical behavior is probably caused by the absence of reflection in the paraxial approximation. The average on-axis power spuriously increases (Fig. 3). However, in nonparaxial theory the opposite happens: the pulse narrows in  $z$  and eventually breaks up into

two main fragments (Fig. 1). The average on-axis power shows an expected decrease (Fig. 3) with propagation length.

In paraxial theory a stable on-axis channel does indeed form (Fig. 2). In [5] it is shown that channel formation can be inferred from the paraxial equation steady in  $z$ , which is cast in the form of a radial eigenvalue problem. Channel formation commences below a critical eigenvalue, which is positive, and the channel width increases as the eigenvalue decreases to zero. Thus the width observed in Fig. 2, which is smaller than the optical wavelength, is consistent with an eigenvalue close to critical. The oscillations in the radial profile of the electron density which are situated outside the channel are observed to have approximately the plasma wavelength. These same oscillations occur in the radial profile of the pulse just outside the channel and are observed to focus and defocus, respectively, with the valleys and peaks of the density as required by refraction. The pulse is indeed contained within the channel and has about a 50-fold increase in intensity over input. However, in nonparaxial theory the beam breaks up (Fig. 1), and the radial pictures corresponding to the same  $z$  point (Fig. 2) show that now the peak intensity is confined in a narrow off-axis trough in the electron density. Thus the beam forms an intense ring around the axis. The ring intensity is reduced about sixfold relative to the paraxial on-axis channel. The nonparaxial on-axis channels (not shown) now exist only in the positions of the on-axis beam remnants shown in Fig. 1. Thus beam breakup has resulted in the formation of ring filaments.

In conclusion, strong relativistic self-focusing is accompanied by wide-angle scattering through  $\pi$  rad such that the paraxial approximation is no longer valid. Wide-angle scattering results in a loss of average on-axis power and eventually leads to beam breakup and filamentation. Future work should examine the reliability of the cycle-average approximation to the plasma dynamics.

The author is grateful to Michael Feit, John Garrison, and Merle Riley for helpful discussion. This work was performed under the auspices of the U.S. Department of Energy by Lawrence Livermore National Laboratory under Contract No. W-7405-ENG-48.

- 
- [1] D. M. Volkov, *Z. Phys.* **94**, 250 (1935); for a review see J. Eberly, in *Progress in Optics*, edited by E. Wolf (North-Holland, Amsterdam, 1969), Vol. 7.
- [2] E. S. Sarachik and G. T. Schappert, *Phys. Rev. D* **1**, 2738 (1970). More recently see J. N. Bardsley, B. M. Penetrante, and M. H. Mittleman, *Phys. Rev. A* **40**, 3823 (1989).
- [3] P. Sprangle, E. Esarey, J. Krall, and G. Joyce, *Phys. Rev. Lett.* **69**, 2200 (1992); E. Esarey, P. Sprangle, J. Krall, and G. Joyce, *Phys. Fluids B* **5**, 2690 (1993); J. Krall, A. Ting, E. Esarey, and P. Sprangle, *Phys. Rev. A* **48**, 2157 (1993); E. Esarey, S. Ride, and P. Sprangle, *Phys. Rev. E* **48**, 3003 (1993).
- [4] S. C. Wilks, W. L. Kruer, M. Tabak, and A. B. Langdon, *Phys. Rev. Lett.* **69**, 1383 (1992); J. Denavit, *ibid.* **69**, 3052 (1992).
- [5] Guo-Zheng Sun, E. Ott, Y. C. Lee, and P. Guzdar, *Phys. Fluids* **30**, 526 (1987).
- [6] A. B. Borisov, A. V. Borovskiy, O. B. Shiryayev, V. V. Korobkin, A. M. Prokhorov, J. C. Solem, T. S. Luk, K. Boyer, and C. K. Rhodes, *Phys. Rev. A* **45**, 5830 (1992).
- [7] A. B. Borisov, A. V. Borovskiy, V. V. Korobkin, A. M. Prokhorov, O. B. Shiryayev, X. M. Shi, T. S. Luk, A. M. McPherson, J. C. Solem, K. Boyer, and C. K. Rhodes, *Phys. Rev. Lett.* **68**, 2309 (1992).
- [8] M. D. Feit and J. A. Fleck, Jr., *J. Opt. Soc. Am. B* **5**, 633 (1988).
- [9] B. Ritchie, *Phys. Rev. A* **45**, R4207 (1992); B. K. Elza and B. Ritchie, *ibid.* **48**, 2940 (1993).
- [10] P. Monot, T. Auguste, L. A. Lompre, G. Mainfray, and C. Manus, *J. Opt. Soc. Am. B* **9**, 1579 (1992).